An assessment of the temporal variability in the annual cycle of daily Antarctic sea ice in the NCAR Community Earth System Model, Version 2: A comparison of the historical runs with observations

Marilyn N. Raphael[1], Mark S. Handcock[1], Marika M. Holland[2], Laura L. Landrum[2]

[1]University of California, Los Angeles
[2]National Center for Atmospheric Research

Key Points:

- Antarctic sea ice extent variability is dominated by sub-decadal variability and that is well represented in the CESM2 simulations.
- The CESM2 simulates an annual cycle of sea ice extent that is comparable in size to that observed but begins its advance and retreat later.
- The later retreat of sea ice in the CESM2 is potentially related to its simulation of the semi-annual oscillation of the circumpolar trough.

Corresponding author: Marilyn N. Raphael, raphael@geog.ucla.edu

Abstract

Understanding the variability of Antarctic sea ice is an ongoing challenge given the limitations of observed data. Coupled climate model simulations present the opportunity to examine this variability in Antarctic sea ice. Here, the daily sea ice extent simulated by the newly-released National Center for Atmospheric Research Community Earth System Model Version 2 (CESM2) for the historical period (1979-2014), is compared to the satellite-observed daily sea ice extent for the same period. The comparisons are made using a newly-developed suite of statistical metrics that estimates the variability of the sea ice extent on timescales ranging from the long-term decadal to the short term, intra-day scales. Assessed are the annual cycle, trend, day-to-day change, and the volatility, a new statistic that estimates the variability at the daily scale. Results show that the trend in observed daily sea ice is dominated by sub-decadal variability with a weak positive linear trend superimposed. The CESM2 simulates this sub-decadal variability with a strong negative linear trend superimposed. The CESM2's annual cycle is similar in amplitude to the observed, a key difference being the timing of ice advance and retreat. The sea ice begins it advance later, reaches its maximum later and begins retreat later in the CESM2. This is confirmed by the day-to-day change. Apparent in all of the sea ice regions, this behavior suggests the influence of the semi-annual oscillation of the circumpolar trough. The volatility, which is associated with smaller scale dynamics such as storms, is smaller in the CESM2 than observed.

Plain Language Summary

Antarctic sea ice is strongly variable in space and in time. Lack of observed data makes it difficult to determine what causes this variability and limits our ability to understand the variability and to project how it might change in the future. Climate models give the opportunity to study the sea ice and to project change. We compare the sea ice simulations produced by the National Center for Atmospheric Research (NCAR) Community Earth System Model Version 2 (CESM2) with satellite-observed data for the years 1979-2014. We examine the annual cycle, trend, day to day change in sea ice and the volatility, a new statistic that estimates the variability at the daily scale. We show that the CESM2 is able to simulate the sub-decadal variability apparent in the observed sea ice but not the weak, positive, linear trend. The CESM2 also simulates an annual cycle of similar amplitude to that observed but the ice starts growing later and retreating later in the CESM2 than is observed. The timing difference in the annual cycle is common to all of the sea ice regions around Antarctica, which suggests that it might be because of a circum-Antarctic atmospheric circulation feature called the circumpolar trough.

1 Introduction

Each year, the total Antarctic sea ice extent (SIE) grows for approximately 225 days to its maximum at the end of winter and retreats for 140 days to its minimum at the end of summer (Handcock & Raphael, 2019), describing what is arguably the most pronounced annual cycle on earth. Embedded within this regularity are regional and temporal variations (e.g., Stammerjohn et al., 2012; Raphael & Hobbs, 2014; Hobbs et al., 2016) that have significance for the Antarctic and global climate. However, aspects of its large scale variability while closely observed, are still not well understood. These include the positive trend in SIE that occurred over the satellite era until 2016 when anomalously early retreat of the sea ice led to record low SIE which continued in subsequent years (*Citations*). There is a critical need for long term data within which to place such variability into context and to provide a basis for projecting future sea ice variability because of the important role that Antarctic sea ice plays in our closely coupled climate system. In the absence of such long term data, coupled climate model simulations present the opportunity to examine this variability in Antarctic sea ice and also to project future

sea ice climate. The models have had some success in simulating the climate. For example, in their analysis of CMIP5 coupled climate models Holmes et al. (2019) have identified one model that exhibits realistic behavior. This model is able to match observations of sea ice drift. They use this to argue that the existing climate models are sophisticated enough to represent aspects of Antarctic sea ice correctly. However, while this is a significant step forward, coupled climate models have had limited success in simulating correctly fundamental aspects of the observed annual cycle and the long term trend. An assessment of the coupled climate models that were contributed to the fifth phase of the Coupled Model Intercomparison Project (CMIP5) found that many of the models had an annual SIE cycle that differed markedly from that observed over the last 30 years (Turner et al., 2013). The majority of models had a SIE that was too small at the minimum in February, while several of the models exhibited much smaller SIE than observed at the September maximum. All of the models had a negative trend in SIE since the mid-twentieth century (contrary to observed) (Turner et al., 2013). For the same suite of models Roach et al. (2018) found that the sea ice concentration (SIC) from which the SIE is calculated was not well represented, for example, being too loose and low-concentration all year. They attribute this to the sea ice thermodynamics used in the models. Antarctic sea ice is intimately tied to the Antarctic climate and these biases in simulated sea ice affect the simulated climate (Bracegirdle et al., 2015). Therefore the inability of the models to simulate historical sea ice correctly limits the confidence that we might have in their projections of future climate.

In this current study we analyze the Antarctic sea ice simulated by the National Center for Atmospheric Research (NCAR) Community Earth System Model Version 2 (CESM2) (Danabasoglu et al., 2020). CESM2 is a fully-coupled, community, global climate model that provides state-of-the-art computer simulations of the Earth's past, present, and future climate states. It is one of the coupled climate models that have contributed to the sixth phase of the Coupled Model Intercomparison Project (CMIP6; Eyring et al., 2016). Other studies have assessed other aspects of the CESM2 Antarctic climate, including the influence of new sea ice physics (Bailey et al., 2020) and variability and predictability characteristics in the pre-industrial climate (Singh et al., 2020). Here we focus on how this model's simulation of Antarctic sea ice compares with observations. Our comparisons focus on the time period 1979 - 2014, which represents a subset of the historical runs which coincides with the bulk of the period of satellite record. We assess the simulations using a suite of statistical metrics developed by Handcock and Raphael (2019) that allow us to to look at the variability on timescales ranging from the long-term decadal to the short term intra-day scales. We focus especially on the annual cycle and the trend, the two most significant components of variability in Antarctic sea ice, and as mentioned above, components which climate models have had difficulty reproducing. The data and method are presented in Section 2, The results are presented and discussed in Section 3 and the work is summarized and conclusions are made in Section 4.

2 Data and Method

Here we use a subset of the CESM2 historical (1850 2014) simulations, 1979 2014, from ten ensemble members and compare it with satellite-observed sea ice data from the Bootstrap Sea Ice Concentrations from Nimbus-7 SMMR and DMSP SSM/I-SSMIS, Version 3 (Comiso, 2017; Peng et al., 2013; Meier et al., 2017) for the same period. The structural details of the CESM2 are elaborated upon in other papers in this CESM2 special collection (Danabasoglu et al., 2020) so are not discussed here.

Daily sea ice extent (SIE) for the CESM2 ensemble mean as well as for the individual ensemble members are compared with the daily SIE from the SSMI data. The SIE is calculated using the limit of the 15% SIC isoline. Thus, it is the sum of the area of every grid cell that is 15% or more covered with sea ice. The use of daily data here is new as previous model comparisons have typically used monthly averaged values. How-

ever, daily data has the potential to give much added information about the sea ice variability simulated by the model at a much finer temporal resolution. Also, much of the variability in contemporary Antarctic sea ice occurs at sub-monthly scales making the examination of daily data particularly useful. For simplicity, most of the discussion of the results focuses chiefly on the model ensemble means.

The components of variability of the SIE that are assessed are the annual cycle, trend, day to day change and the *volatility*. Comparisons to the long term trends may be challenging due to the role of internal variability (e.g., Polvani & Smith, 2013; Mahlstein et al., 2013). However, looking across multiple ensemble members allows some insight on whether the model can simulate a combination of external forcing and internal variability that is comparable to observations. While the annual cycle and trend are the two components most usually assessed, the day to day change and the volatility are new. This is largely because most analyses have been conducted on monthly or seasonal averages. The volatility is a new metric developed in Handcock and Raphael (2019). The sea ice record on any given day is the sum of a number of components of variation the interannual variation, the annual cycle for that day, day to day variation and the volatility (or statistical error) in the observed daily value. Normally that error is considered or represented as a constant over time. However, here, we allow it to vary, explicitly representing it as a calendar time varying component. We define it as the daily standard deviation which is the intra-day uncertainty in the sea ice extent. The volatility in observed data is considered to be due largely to factors like the ephemeral dynamics effects of storms at the ice edge and wave-ice interactions. Some, smaller, portion of it may be due also to instrumentation and algorithm effects.

Antarctic sea ice distribution varies regionally, therefore our analyses examines the total SIE as well as the regional SIE variability in order to get a comprehensive sense of the model's performance. The sea ice regions used in this analysis were defined by Raphael and Hobbs (2014) and are based on coherent spatial variability in the sea ice concentration field. DuVivier et al. (2019) assesses the seasonal distribution of sea ice concentration simulated by the CESM2. Their Figure 13 shows that the model does a credible job of simulating the concentration of sea ice. Antarctic sea ice variability is closely tied to the variability in sea level pressure (SLP) over the Southern Ocean. Using SLP, taken from the ERA-Interim Reanalyses for the period 1979 - 2014, we make a preliminary diagnosis of reason for the differences between the simulated and observed SIE. We compare the simulated SLP with the corresponding variable in the ERA-Interim dataset.

3 Results

3.1 Trend

It is common in climate science to represent variability at sub-decadal or longer timescales as linear functions of time. In this case the presence of a non-zero slope is evidence of change. Here we expand the representation to allow non-linear functions of time, specifically slowly changing curvilinear functions of time. This allows more flexible and realistic representations of change while retaining linear trends as a special case. Our trend is explicitly defined in equation (15) of Handcock and Raphael (2019). As we show below, this curvilinear trend captures variability at sub-decadal timescales.

Very few climate models that participated in the previous CMIPs have been able to simulate the observed positive linear trend in Antarctic SIE that occurred from 1979-2016 (e.g., Turner et al., 2013; Shu et al., 2015). One suggested reason for this discrepancy is the possibility that the processes underlying the increase in sea ice extent are not correctly represented in the models (e.g., Turner et al., 2013; Sigmond & Fyfe, 2014). Another is that the observed increase in sea ice extent might be due to natural variability rather than external forcing in the system and therefore, that the climate models do

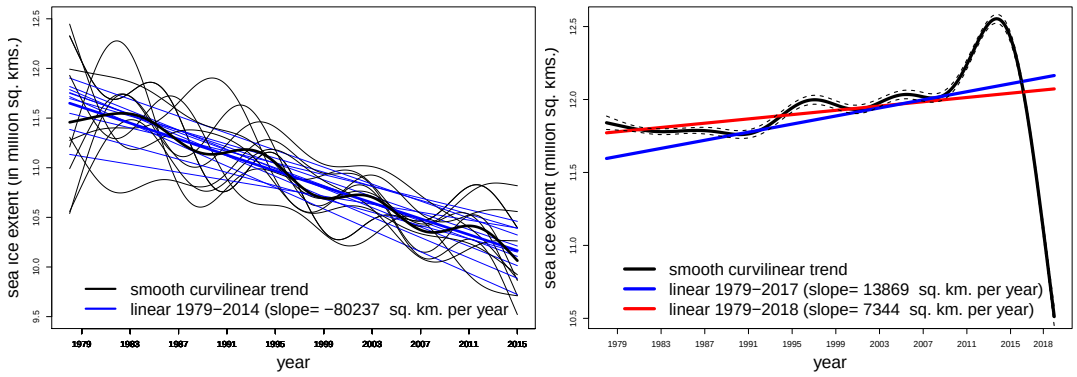

(a) (b)

Figure 1. Observed and simulated trends in daily Antarctic sea ice extent represented in terms of the area of sea ice involved in the trend. a) Curvilinear (black) and linear (blue) trends simulated by the CESM2. Bold lines are the ensemble mean, thin lines are the individual ensemble members; b) Observed trends in daily Antarctic sea ice linear trend from 1979 2017 (blue), from 1979 2018 (red); curvilinear trend (black) with 95% pointwise confidence intervals (dashed black lines).

not simulate it is not necessarily a failure of the models (e.g., Polvani & Smith, 2013; Mahlstein et al., 2013). Figure 1a, which shows change in SIE associated with the trend, illustrates that as was the case for the majority of the CMIP5 models, this most recent version of CESM2 simulates a pronounced negative linear trend (thick orange line). This is true in the ensemble mean and also apparent in each ensemble member. However, Figure 1b which shows the observed daily linear trend in total Antarctic SIE demonstrates that this observed positive linear trend is quite weak and may be strongly influenced by the record maxima which occurred from 2012 2014. Interestingly, Figure 1b also suggests that this level of variability of daily SIE is better represented as a curvilinear function of time rather than a linear one, suggesting variability at sub-decadal timescales. The linear trend does not provide a good characterization of the data because of these sub-decadal variations. The CESM2 captures the sub-decadal variability (Figure 1a, black lines), indeed the simulated version is much more pronounced than observed. The sub-decadal variability in the daily SIE in this analysis is consistent with that discussed by Simpkins et al. (2013) in their analysis of changes in the magnitudes of the sea ice trends in the Ross and Bellingshausen Seas. That the CESM2 is successful at capturing the sub-decadal variability in the SIE suggests that the model may be used for diagnosing the mechanisms that force this nonlinear behavior.

We also examine the simulated trend by region (Figure 2). Figure 2b shows the ensemble mean simulated trends. The curvilinearity apparent in the total SIE is also noted regionally. The largest changes are in the Ross, Weddell and King Hakon sectors, followed by East Antarctica and the Amundsen-Bellingshausen (ABS) sectors. It is interesting to note that the timing of the subdecadal variation is not synchronous in some regions, a fact best illustrated by the Ross and Weddell Sea sectors (Figure 2a&b). This dipole of variability between the Weddell and Ross sectors is reminiscent of the Antarctic Dipole, the leading mode of interannual variability in Antarctic sea ice (e.g., Yuan & Martinson, 2000, 2001; Holland et al., 2005). Given that these two sectors contribute most to the total SIE, such lack of synchronicity would have a significant effect on the

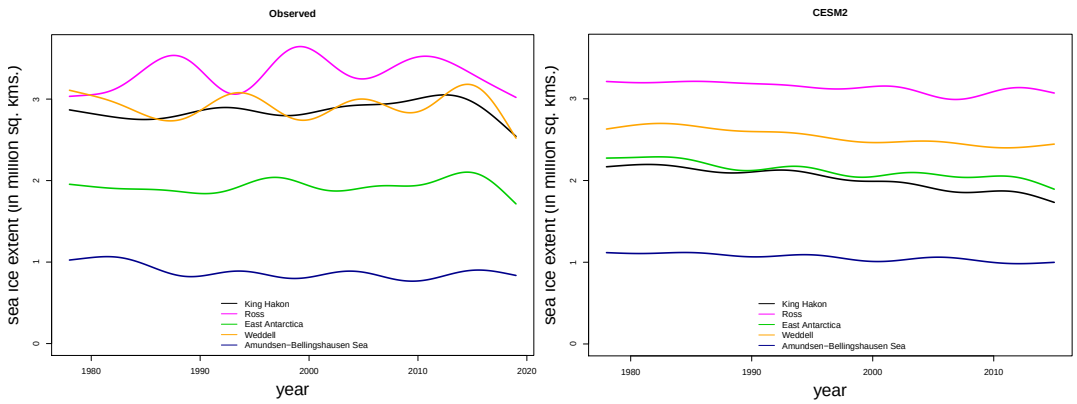

Figure 2. Regional observed and simulated trends in daily Antarctic sea ice extent. a) Observed trends; b) Trends simulated by the CESM2. Regions are Amundsen-Bellingshausen sector (dark blue), East Antarctica (green), Weddell Sea (orange), King Hakon VII (black); Ross Sea (magenta)

trend in total SIE. Regionally, the CESM2 captures the range of the trends in terms of the area of sea ice involved. As is observed, the simulated ABS sector has the smallest effect while the Ross Sea sector has the largest in terms of the area of sea ice. The trend in the King Hakon sector is weaker and now comparable to the neighboring East Antarctica sector. The curvilinearity in the time-series is apparent at the regional scale but weaker in general than observed. A good proportion of this is due to averaging the curvilinearity of the ensemble members, however, calculations of the average variance of the curvilinearity of ensemble members shows that the Ross, Weddell and Amundsen-Bellingshausen sectors have lower variance than the observed, while the King Hakon and East Antarctica exhibit more.

3.2 Annual cycle

Here we compare the amplitude (the difference between the maximum and minimum extents), and phase (the timing of the advance and retreat) of the observed, daily annual cycle of SIE with that simulated by CESM2. The amplitude and phase are the two key characteristics of the annual cycle of sea ice. The traditional way of calculating the annual cycle is to take the average SIE for each day of the year. However, an annual cycle produced in this fashion does not include the effect of the day preceding nor the day following the averaged day, therefore it disguises the fact that the phase may be changing slowly and that the amplitude and shape of the annual cycle might vary. Given these limitations we calculate an annual cycle that is adjusted for amplitude and phase. The mathematical detail of the calculations is specified in Handcock and Raphael (2019), Section 3.1. It assumes that the amplitude varies annually while the phase, which is the timing of advance and retreat of the ice, varies continuously. In this way, the annual cycle is not constrained to be a fixed (in time) cyclical pattern. Instead, the amplitude and shape of the cycle are allowed to vary, as would occur naturally. The outcome, averaged over the dataset period, is shown in Figure 3a and presents a more thorough if nuanced description of the annual cycle than the traditional daily climatology. For clarity, Figure 3 shows only the ensemble mean and the observed cycles. On the horizontal axis is the day of the cycle not the day of year. Day 1, which is the average day on which the

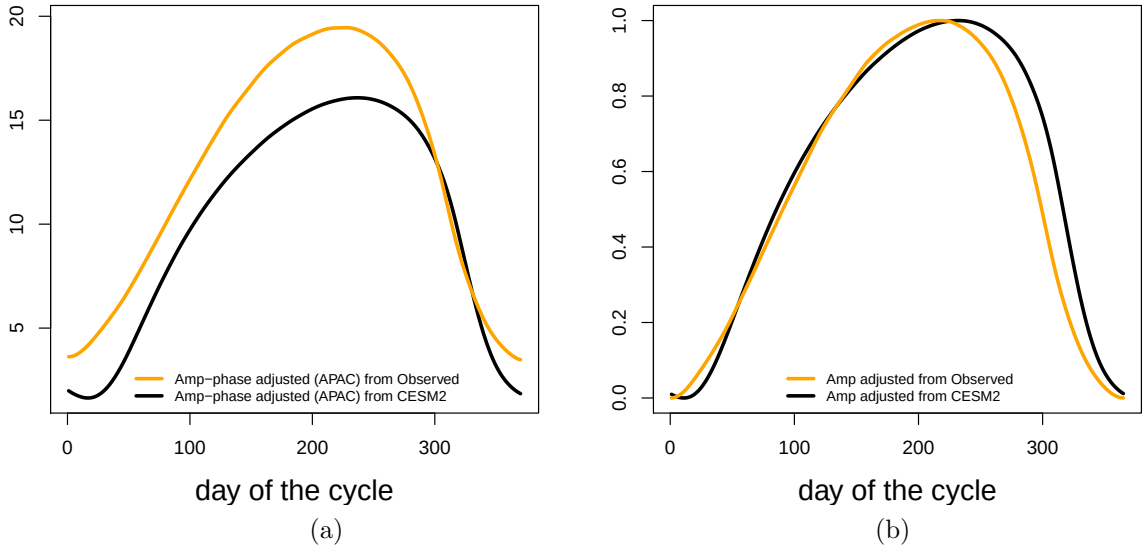

Figure 3. Observed and simulated annual cycles. a) Amplitude and phase adjusted annual cycles; b) Amplitude adjusted only annual cycles. CESM (black lines), Observed (orange lines). On the horizontal axis is day of cycle day 0 is Julian Day 50. On the vertical axis is sea ice extent in millions of square kilometers.

sea ice stops retreating and begins to advance is Julian day 50. Figure 3a shows that the simulated SIE is much smaller than the observed, especially at sea ice minimum and maximum. This result is similar to what was found in previous studies (e.g., Turner et al., 2013). Moreover, it shows clearly that the sea ice minimum in the model occurs after ice has begun its advance in the observed cycle and there are small differences during the retreat phase of the ice. Given that the annual cycle in the model is starting later and from a lower minimum it is possible that the model is simulating an amplitude, i.e a difference between the SIE at maximum and minimum, that is within range of that observed.

To examine more closely the similarity in amplitude and differences in timing shown on Figure 3a, we calculate an amplitude-adjusted annual cycle which standardizes the variation in amplitude while allowing variation in phase. Details of its calculation are also specified in Handcock and Raphael (2019), Section 3.1. Figure 3b shows that there are phase differences between the CESM2 and the observed annual cycles, most obviously in the retreat period. In the advance period, the sea ice in CESM2 begins advancing some days later than the observed but catches up quickly and the rate of advance appears to be more or less the same for most of the growth phase of the ice. There is however, a clear difference in phase for the latter part of the ice cycle. During this time, the observed sea ice begins to retreat at day of cycle 215 (Julian Day 266), 12 days earlier than the CESM2 ensemble mean simulations. To put this in recent context, the anomalously early retreat of sea ice in 2016 began approximately three weeks before the median retreat onset. This points to the benefit of using daily data, as these differences would not be adequately resolved using monthly means.

This difference in phase is also seen in Figure 3a but not as clearly as that effect is dominated by the apparent amplitude difference. The amplitude-only adjusted annual cycles are also examined for each region (Figure 5). While there are regional differences in the shape and length of the annual cycle which may be interesting to explore, they all have in common the phase difference seen in the total SIE. That is, sea ice begins to retreat later in the model than observed in each of the regions. The sea ice regions are

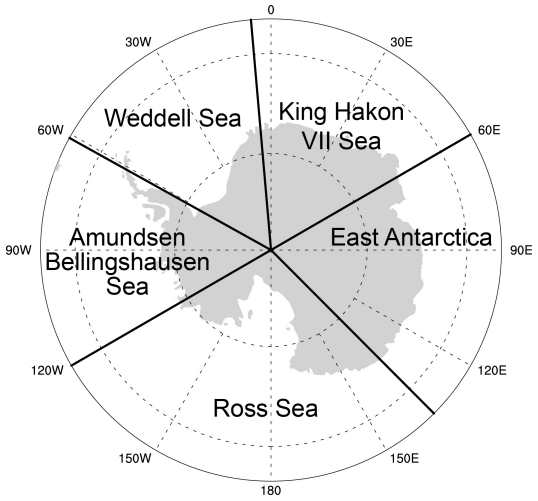

Figure 4. Sea Ice Regions around Antarctica. Based on Raphael and Hobbs (2014).

shown in Figure 4. That the difference in phase is consistent in all of the regions around the continent suggests that it is due to a large-scale rather than regional mechanism. A potential agent is the semi-annual oscillation (SAO) of the circumpolar trough (CPT). Earlier studies suggest that the SAO modulates the advance and retreat of the ice because it influences the location of the westerly and easterly surface winds which in turn promote or limit the spread of the ice (e.g., Enomoto & Ohmura, 1990; Stammerjohn et al., 2003). This is explored below.

3.3 Day to day change in SIE

The simulated day to day change in SIE has not been compared with observed data before. However, as Figure 6a shows, it can yield information that explains the differences that exist in the annual cycles. As shown by the ensemble mean, the simulations capture the general shape of the day to day changes in ice but there are important differences. SIE in the CESM2 starts advancing later, from a lower value, achieves its peak growth rate earlier, and has a maximum growth rate that is higher than the observed. Once its peak growth rate is achieved, it continues to grow more slowly for the rest of its advance. It achieves its maximum later and begins retreat later, achieving a rate of retreat that is faster and later in the cycle than is observed. The day to day change is consistent with the annual cycles shown in Figure 3, especially with the phase differences seen in Figure 3b. Additionally, it suggests that the very low minimum achieved by the CESM2 is related to the high, late stage, maximum decay rate.

Regionally, the day to day changes display grossly similar characteristics to the total SIE but there are some differences (Figure 6b - f). While the exact timing of the start of retreat varies by region, the sea ice retreat begins later in CESM2 in each region. The maximum rate of retreat also occurs later in CESM2; this is most pronounced in the East Antarctica sector, least, in the Weddell Sea. The Weddell Sea sector is most similar to the observed while the King Hakon sector is the most different; its growth and retreat rates are lower than observed. The East Antarctica and Ross sectors are in phase with the observed but have later and greater maximum rate of decrease. Overall the regional day to day changes are consistent with the regional phase differences seen in the amplitude-only adjusted annual cycles in Figure 5.

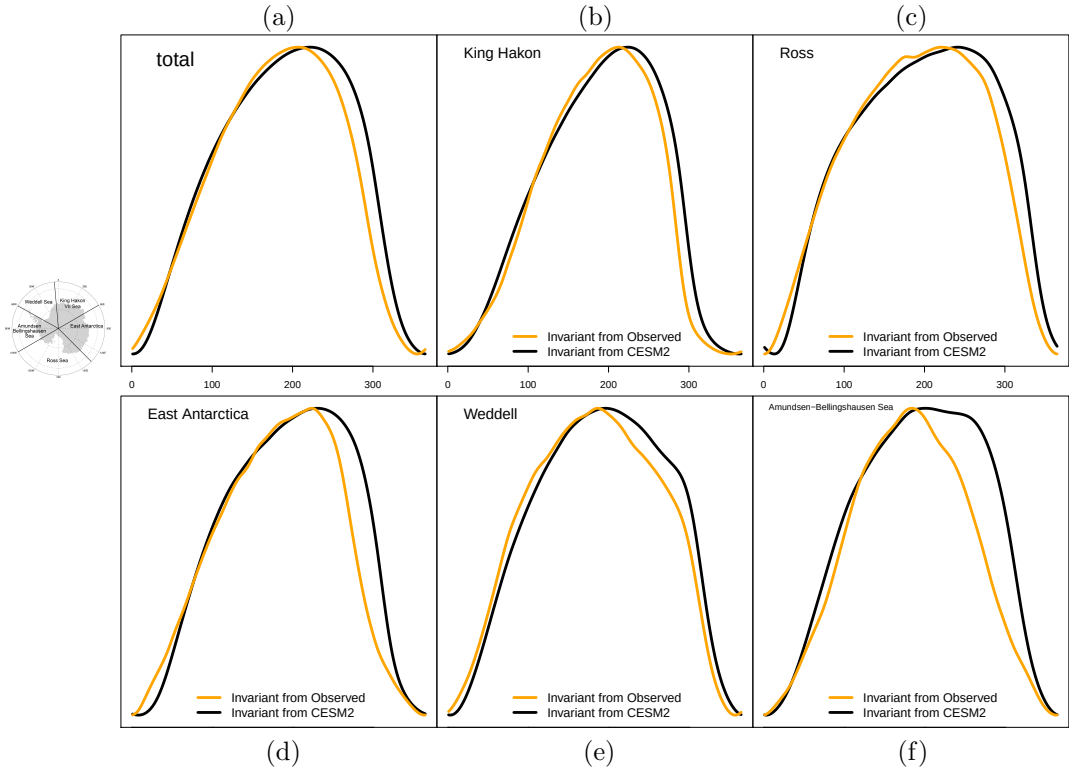

Figure 5. Regional observed and simulated invariant annual cycles. a) Total sea ice extent. b) King Hakon VII, c) Ross Sea, d) East Antarctica, e) Weddell Sea, f) Amundsen-Bellingshausen Sea. On the horizontal axis is day of cycle day 0 is Julian Day 50. On the vertical axis is sea ice extent in millions of square kilometers.

3.4 Volatility

The sea ice volatility, the daily standard deviation in the sea ice simulated by the coupled climate models, has not been evaluated before. However, as shown in Figure 7, the volatility can be responsible for fluctuations at the ice edge on the order of 40,000 50,000 km^2 which, while small compared to the total SIE, becomes significant at the regional scale and when compared to the size of the sea ice grid box. Overall, the volatility of CESM2 is lower than the observed by approximately 20,000 km^2 per day. The volatility in the observed data is lowest during the early stages of ice advance, large at SIE maximum and achieves a second, larger maximum later in the cycle, during the days of fastest sea ice retreat. By comparison, the CESM2 volatility increases early during ice advance, maintains a steady state for most of the year and like the observed, experiences a large maximum late in the ice cycle. The peak in volatility late in the cycle must be related to the maximum decay rate in the ice since in both the observed and the ensemble mean it occurs at approximately the same time as the peak rates of decay shown in Figure 6. Regionally (Figure 7), volatility is usually lower in CESM2 except during retreat in the ABS and East Antarctica. The late cycle increase in volatility occurs in all of the regions, except the ABS, and coincides with the time of maximum decay.

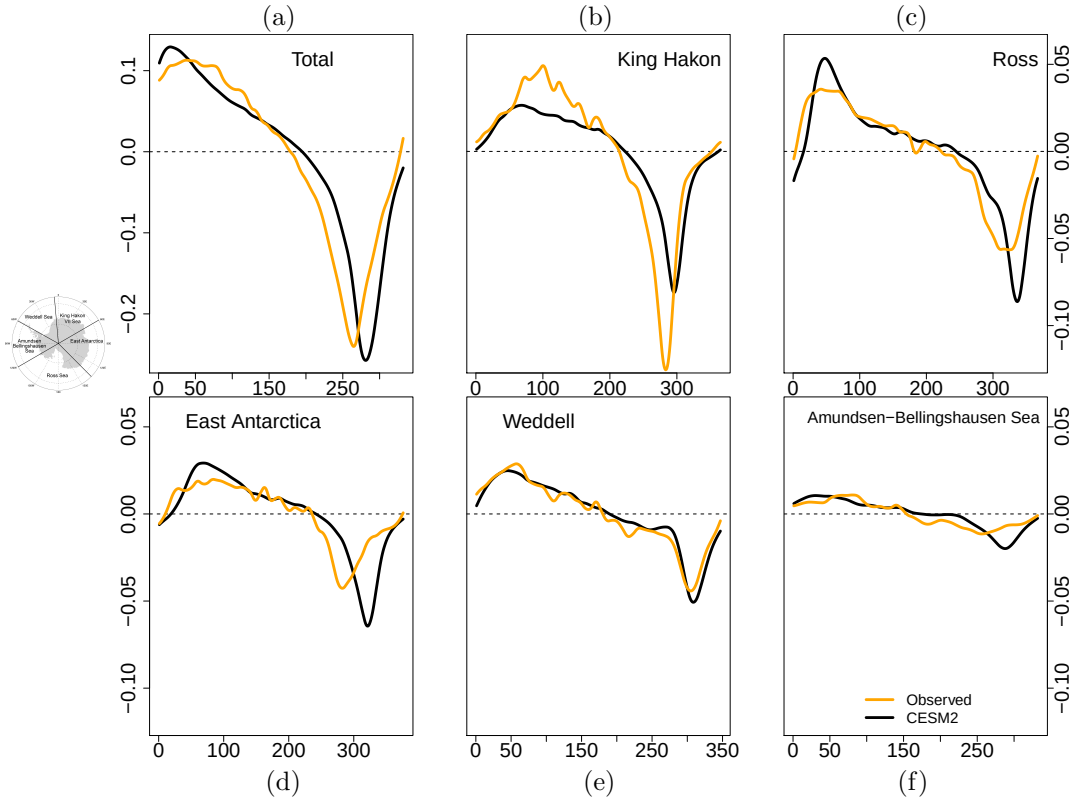

Figure 6. Total and Regional observed (orange) and simulated (black) day to day change in Antarctic sea ice. a) Total sea ice extent. b) King Hakon VII, c) Ross Sea, d) East Antarctica, e) Weddell Sea, f) Amundsen-Bellingshausen Sea. On the horizontal axis is day of cycle day 0 is Julian Day 50. On the vertical axis is sea ice extent in millions of square kilometers.

The volatility in the observed data is considered to be due mainly to the dynamic effects of storms, ocean circulation (eddies) and wave-ice interaction at the ice edge. Stammerjohn et al. (2003) suggest that dynamics rather than thermodynamics initiate and dominate anomalies along the ice edge. There is a peak in storm activity in the southern winter (e.g., Carleton, 1979; Simmonds & Keay, 2000). These storms cause fluctuations at the sea ice edge rather than within the pack where the sea ice concentration is at or close to 100%. Therefore, the apparent cycle in volatility may be due to the effect of storms at the ice edge. The lower volatility exhibited by the CESM2 during most of the growth stage of the ice, suggests that dynamic forcing of ice fluctuation at the ice edge in the CESM2 is smaller than observed. This can happen if the processes that drive high frequency variability inherent in features such as storms and ocean eddies, are deficient in the model, which is a likely consequence of the relatively coarse model resolution (of about 1 degree in latitude and longitude).

3.5 The Potential role of the Semi-annual Oscillation

Integrating the information given by the comparison of the annual cycles, the day to day mean and the volatility we see that the CESM2 simulates an annual cycle with amplitude similar to that observed but with a retreat phase that begins later in the cycle. We also see that the simulated maximum decay rate is greater, occurs later in the

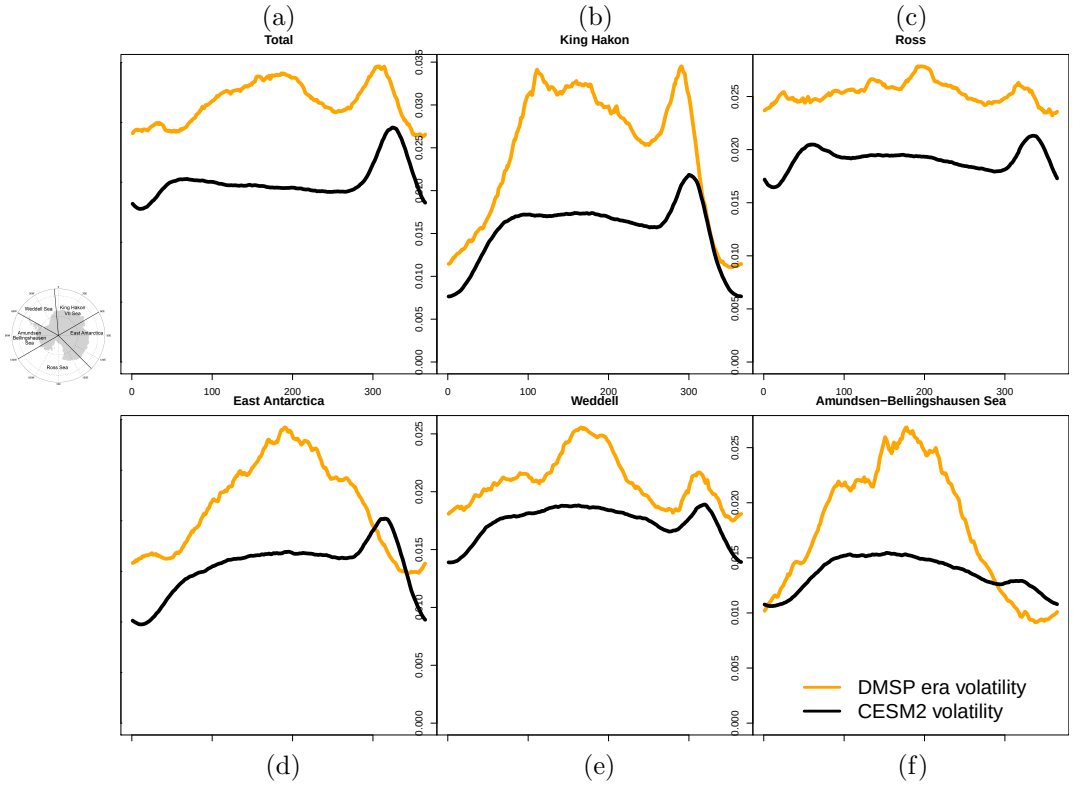

Figure 7. Regional observed (orange) and simulated (black) volatility in Antarctic sea ice. a) Total sea ice extent. b) King Hakon VII, c) Ross Sea, d) East Antarctica, e) Weddell Sea, f) Amundsen-Bellingshausen Sea. On the horizontal axis is day of cycle day 0 is Julian Day 50. On the vertical axis is sea ice extent in millions of square kilometers.

cycle, and is associated with the late peak in volatility. We address now a factor that moderates the timing or phase of the annual cycle, the semi-annual oscillation (SAO). Although it has not been fully quantified, a number of studies suggest that the timing of advance and retreat of Antarctic sea ice is moderated by the SAO (Enomoto & Ohmura, 1990; Simmonds, 2003; Stammerjohn et al., 2003; Simmonds et al., 2005). An important characteristic of the southern hemisphere atmospheric circulation, the SAO is associated with more than 50% of the variability in SLP (Van Loon & Rogers, 1984; Taschetto et al., 2007). It is expressed by the bi-annual changes in location and intensity of the circumpolar trough (CPT). As described in van Loon (1967), the CPT contracts, deepens and moves south in March and September and expands, weakens and moves north in June and December. Similar accompanying fluctuations of the tropospheric temperature gradients, geopotential heights, SLP and winds at middle and high latitudes in the SH occur. The changing wind directions associated with the meridional shift in the CPT in spring is thought to create divergence in the ice pack causing a reduction in sea ice concentration and priming the pack for rapid break up by wind and ocean late in the annual cycle (December) (Enomoto & Ohmura, 1990). Stammerjohn et al. (2003) show that the timing of the north/south migration of the CPT influences the timing of sea-ice advance and retreat via wind-driven sea-ice drift. A lucid discussion of the SAO and its influence on Antarctic sea ice can be found in Eayrs et al. (2019).

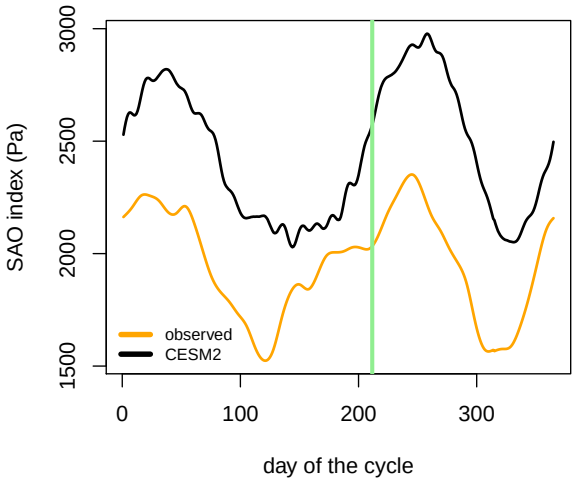

Figure 8. Semi-annual Oscillation Index: Observed (orange) and simulated (black) zonal mean SLP difference between latitudes 50S and 65S. The green line marks the observed day of onset of sea ice retreat. On the horizontal axis is day of cycle day 0 is Julian Day 50. On the vertical axis is the zonal mean sea level pressure difference in Pa.

An in depth evaluation of SAO simulated by the CESM2 within the context of sea ice variability is beyond the scope of this paper. However, given the hypothesized link between the SAO and the timing of sea ice advance and retreat, and its potential for explanation, we examined how well the CESM2 simulates the SAO, using the zonal mean SLP difference between latitudes 50S and 65S. It is a measure of the strength of the winds between those latitudes such that a large, positive value indicates stronger westerlies, and the intensity of the CPT (Hurrell & Van Loon, 1994; Meehl et al., 1998; Taschetto et al., 2007). CESM2 (Figure 8: black line) simulates a well-defined SAO index which is different from the observed in two ways; it is always larger, indicating stronger winds and a deeper CPT, and it is offset in time so that the minimum and maximum meridional pressure gradients are achieved later in the year than observed. This means that the simulated CPT begins shifting southwards later, reaching its southernmost location and greatest intensity later than the observed CPT. The significance of this temporal offset to the timing of ice retreat becomes clearer in Figure 9a and b where the day to day changes in SIE are overlaid on the observed and simulated SAO indices along with the times of onset of retreat. The later retreat of ice in the CESM2 is tied to the slower southward movement of the CPT.

4 Summary and Conclusions

This study is an evaluation of the satellite-era variability in Antarctic sea ice extent simulated by the CESM2, using some newly developed metrics from Handcock and Raphael (2019). These metrics examine the variability from the long term trends to the intra-day, giving a detailed picture of the temporal variability of Antarctic sea ice extent simulated by the model. This complements work that has assessed other aspects of the Antarctic climate in pre-industrial control conditions (Singh et al., 2020). Here, we are able to explicitly diagnose differences between the model and observed, which may be used to give a sense of what elements of the model need more development. Over the historical period the trend in observed daily sea ice is dominated by a curvilinear interannual component with a weak positive linear trend superimposed. As was the case for the majority of the CMIP5 models, CESM2 simulates a strong negative trend in SIE and therefore is still in contrast to the observations, a difference which might be due to nat-

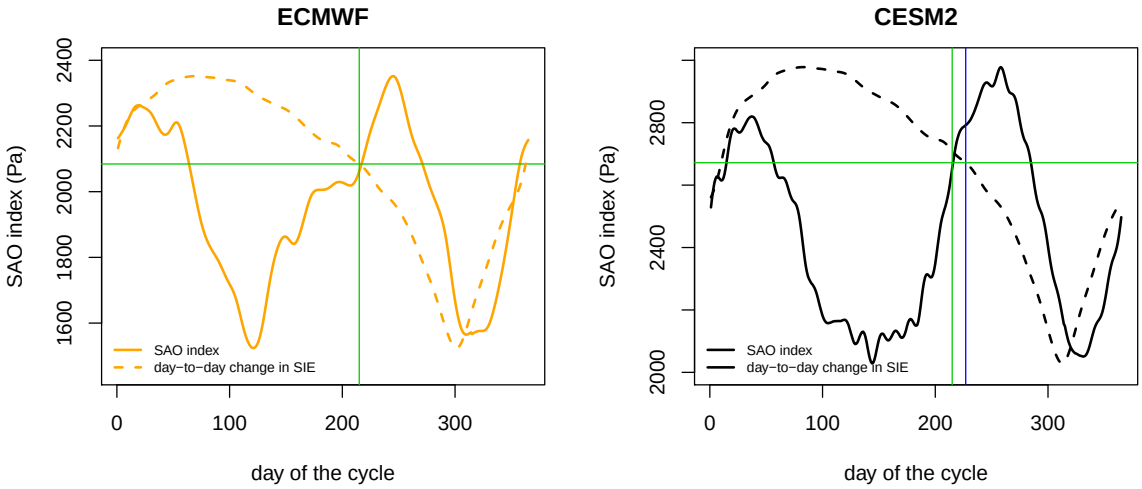

Figure 9. Observed (a) and simulated (b) day to day change and corresponding SAO index. The green line marks the observed day of onset of sea ice retreat. The blue line marks the simulated day of onset of sea ice retreat. On the horizontal axis is day of cycle: day 0 is Julian Day 50. On the vertical axis is the zonal sea level pressure difference in Pa.

ural variability rather than a model deficiency. However, very importantly, the CESM2 captures the inter-annual component or sub-decadal variability in both the total SIE and the individual sea ice sectors. This suggests that the CESM2 could be used to evaluate/diagnose the factors contributing to this trend.

With respect to the annual cycle, the total SIE at time of maximum simulated by the CESM2 is lower than recorded. This low value might be attributed in part to the strong and consistent negative trend in sea ice simulated by the model. It is also clear that sea ice in the model begins growing from a smaller minimum and thus might never reach the size of the observed at the time of maximum. However, if the amplitude is calculated as the difference between the minimum and maximum SIE, the CESM2 does produce an annual cycle with similar amplitude to that observed. The key difference between the simulated and observed annual cycles is the timing of ice retreat. The CESM2 reaches its SIE maximum later and begins its retreat later than observed and this is apparent in both the total and the regional SIE.

This difference in the annual cycles is echoed in the day-to-day change, a variable that has not been examined before since most analyses focus on the monthly and seasonal SIE. Here, the day-to-day change is consistent with and might be considered a proxy for the large scale elements of the annual cycle (advance/retreat), while adding precision with respect to the exact timing of advance and retreat. While the rates of change are generally similar (except for the peak rate of retreat in the CESM2 which is much larger), sea ice begins its advance and retreat later in the CESM2.

A potential contributor to this phase difference is the simulated semi-annual oscillation (SAO). An initial evaluation of the SAO index shows that the meridional gradient of pressure simulated by the CESM2 is larger and the maximum (and minimum) of this gradient occur later in the cycle than observed. It is suggested that this is due to a deeper, slower moving CPT. The influence of the SAO on sea ice variability has long been a subject of study (e.g., Van Den Broeke, 2000). These differences between the CESM2 and the observed data present an opportunity to examine closely, this important atmospheric mechanism and its role in the Antarctic sea ice climate.

A final aspect of variability compared is the daily standard deviation, named here, the volatility (Handcock & Raphael, 2019). In general, this component of variability is lower in the CESM2 than observed. Also missing is the slow but clear growth in volatility to a maximum near the time of the sea ice maximum. However, the CESM2 captures the peak volatility associated with the very rapid rate of decay late in the ice cycle that is also apparent in the observed data. As mid-winter sea ice variability is associated with the smaller scale dynamics such as storms (e.g., Stammerjohn et al., 2003), ocean eddies and wave-ice interaction at the ice edge it may be that the model is not simulating these processes well, something that is common across the CMIP models. We note also that the observed sea ice grid size at 25km x 25km is much smaller than that of the CESM2's (1 degree) thus might be expected to exhibit more daily volatility than the CESM which is a 1 degree model.

Acknowledgments

The CESM project is supported primarily by the National Science Foundation (NSF). This material is based upon work supported by the National Center for Atmospheric Research, which is a major facility sponsored by the NSF under Cooperative Agreement No. 1852977. Computing and data storage resources, including the Cheyenne supercomputer (doi:10.5065/D6RX99HX), were provided by the Computational and Information Systems Laboratory (CISL) at NCAR. We thank all the scientists, software engineers, and administrators who contributed to the development of CESM2. LL was funded by NSF grant 1643484.

The CESM2 model output used in this study is available at the NCAR Digital Asset Services Hub (DASH; https://data.ucar.edu) The Bootstrap Sea Ice Concentration data are available at the National Snow and Ice Data Center. Bootstrap Version 3 concentration fields (Comiso, 2017) from the "NOAA/NSIDC Climate Data Record of Passive Microwave Sea Ice Concentration, Version 3". The ERAI reanalysis data are available from ECMWF at `http://apps.ecmwf.int/datasets/data/interim_full_daily`

References

Bailey, D. A., Holland, M. M., DuVivier, A. K., Hunke, E. C., & Turner, A. K. (2020). *Impact of a new sea ice thermodynamic formulation in the CESM2 sea ice component.* (Manuscript submitted for publication to the *Journal of Advances in Modeling Earth Systems*)

Bracegirdle, T. J., Stephenson, D. B., Turner, J., & Phillips, T. (2015). The importance of sea ice area biases in 21st century multimodel projections of antarctic temperature and precipitation, geophys. *Geophysics Research Letters*, *42*(10), 832-839. doi: 10.1002/2015GL067055

Carleton, A. M. A. (1979). synoptic climatology of satellite-observed extratropical cyclone activity for the southern hemisphere winter. *Archives for meteorology, geophysics, and bioclimatology*, *27*, 265-279.

Comiso, J. (2017). *Bootstrap sea ice concentrations from NIMBUS-7 SMMR and DMSP SSM/I-SSMIS, Version 3.* NASA National Snow and Ice Data Center Distributed Active Archive Center. doi: 10.5067/7Q8HCCWS4I0R

Danabasoglu, G., Lamarque, J.-F., Bacmeister, J., Bailey, D. A., DuVivier, A. K., Edwards, J., ... Strand, W. G. (2020). The community earth system model Version 2 (CESM2). *Journal of Advances in Modeling Earth Systems*, *12*(2), e2019MS001916. doi: 10.1029/2019MS001916

DuVivier, A. K., Holland, M. M., Kay, J. E., Tilmes, S., Gettelman, A., & Bailey, D. A. (2019). *Arctic and antarctic sea ice state in the community earth system model version 2.* Manuscript submitted to JGR-Oceans.

Eayrs, C., Holland, D. M., Francis, D., Wagner, T. J. W., Kumar, R., & Li, X. (2019). Understanding the seasonal cycle of antarctic sea ice extent in the

context of longerterm variability. *Reviews of Geophysics*, *57*, 1037-1064.

Enomoto, H., & Ohmura, A. (1990). The influences of atmospheric half-yearly cycle on the sea ice extent in the antarctic. *Journal of Geophysical Research: Oceans*, *95*(C6), 9497-9511. doi: 10.1029/JC095iC06p09497

Eyring, V., Bony, S., Meehl, G. A., Senior, C. A., Stevens, B., Stouffer, R. J., & Taylor, K. E. (2016). Overview of the coupled model intercomparison project phase 6 (cmip6) experimental design and organization. *Geoscientific Model Development*, *9*(5), 1937–1958. doi: 10.5194/gmd-9-1937-2016

Handcock, M. S., & Raphael, M. N. (2019). Modeling the annual cycle of daily antarctic sea ice extent. *The Cryosphere Discussions*, *2019*, 1–19. doi: 10 .5194/tc-2019-203

Hobbs, W. R., Massom, R., Stammerjohn, S., Reid, P., Williams, G., & Meier, W. (2016, August). A review of recent changes in Southern Ocean sea ice, their drivers and forcings. *Global and Planetary Change*, *143*, 228-250. doi: 10.1016/j.gloplacha.2016.06.008

Holland, M. M., Bitz, C. M., & Hunke, E. C. (2005). Mechanisms forcing an antarctic dipole in simulated sea ice and surface ocean conditions. *Journal of Climate*, *18*(12), 2052-2066. doi: 10.1175/JCLI3396.1

Holmes, C. R., Holland, P. R., & Bracegirdle, T. J. (2019). Compensating biases and a noteworthy success in the CMIP5 representation of antarctic sea ice processes. *Geophysical Research Letters*, *46*, 4299-4307.

Hurrell, J. W., & Van Loon, H. (1994). A modulation of the atmospheric annual cycle in the southern hemisphere. *Tellus*, *46A*, 325-338.

Mahlstein, I., Gent, P. R., & Solomon, S. (2013). Historical antarctic mean sea ice area, sea ice trends, and winds in CMIP5 simulations. *Journal of Geophysical Research: Atmospheres*, *118*(11), 5105-5110. doi: 10.1002/jgrd.50443

Meehl, G. A., Hurrell, J. W., & H. van Loon, A. (1998). modulation of the mechanism of the semiannual oscillation in the southern hemisphere. *Tellus*, *50A*, 442-450.

Meier, W. N., Fetterer, F., Savoie, M., Mallory, S., Duerr, R., & Stroeve, J. (2017). NOAA/NSIDC climate data record of passive microwave sea ice concentration, version 3 [Computer software manual]. Boulder, Colorado USA. doi: https://doi.org/10.7265/N59P2ZTG

Peng, G., Meier, W. N., Scott, D. J., & Savoie, M. H. (2013). A long-term and reproducible passive microwave sea ice concentration data record for climate studies and monitoring. *Earth System Science Data*, *5*(2), 311–318. doi: 10.5194/essd-5-311-2013

Polvani, L. M., & Smith, K. L. (2013). Can natural variability explain observed antarctic sea ice trends? new modeling evidence from CMIP5. *Geophysical Research Letters*, *40*(12), 3195-3199. doi: 10.1002/grl.50578

Raphael, M. N., & Hobbs, W. (2014). The influence of the large-scale atmospheric circulation on antarctic sea ice during ice advance and retreat seasons. *Geophysical Research Letters*, *41*, 5037-5045. doi: 10.1002/2014gl060365

Roach, L. A., Dean, S. M., & Renwick, J. A. (2018). Consistent biases in antarctic sea ice concentration simulated by climate models. *The Cryosphere*, *12*, 365-383.

Shu, Q., Song, Z., & Qiao, F. (2015). Assessment of sea ice simulations in the CMIP5 models. *The Cryosphere*, *9*(1), 399–409. doi: 10.5194/tc-9-399-2015

Sigmond, M., & Fyfe, J. C. (2014). The antarctic sea ice response to the ozone hole in climate models. *Journal of Climate*, *27*(3), 1336-1342. doi: 10.1175/JCLI-D -13-00590.1

Simmonds, I. (2003). Modes of atmospheric variability over the southern ocean. *Journal of Geophysical Research: Oceans*, *108*(C4), SOV 5-1-SOV 5-30. doi: 10.1029/2000JC000542

Simmonds, I., & Keay, K. (2000, March). Mean Southern hemisphere extratropical

cyclone behavior in the 40-year NCEP-NCAR reanalysis. *Journal of Climate*, *13*, 873-885. doi: 10.1175/1520-0442(2000)013⟨0873:MSHECB⟩2.0.CO;2

Simmonds, I., Rafter, A., Cowan, T., Watkins, A. B., & Keay, K. (2005, October). Large-scale Vertical Momentum, Kinetic Energy and Moisture Fluxes in the Antarctic Sea-ice Region. *Boundary-Layer Meteorology*, *117*(1), 149-177. doi: 10.1007/s10546-004-5939-6

Simpkins, G. R., Ciasto, L. M., & England, M. H. (2013). Observed variations in multidecadal antarctic sea ice trends during 1979–2012. *Geophysical Research Letters*, *40*(14), 3643-3648. doi: 10.1002/grl.50715

Singh, H. K. A., Landrum, L., & Holland, M. M. (2020). *An overview of antarctic sea ice in the CESM2: Analysis of the seasonal cycle, predictability, and atmosphere-ocean-ice interactions.* (Manuscript submitted for publication to the *Journal of Advances in Modeling Earth Systems*)

Stammerjohn, S., Drinkwater, M. R., Smith, R. C., & Liu, X. (2003). Ice-atmosphere interactions during sea-ice advance and retreat in the western antarctic peninsula region. *Journal of Geophysical Research: Oceans*, *108*(C10). doi: 10.1029/2002JC001543

Stammerjohn, S., Massom, R., Rind, D., & Martinson, D. (2012). Regions of rapid sea ice change: An inter-hemispheric seasonal comparison. *Geophysical Research Letters*, *39*(6). doi: 10.1029/2012GL050874

Taschetto, A., Wainer, I., & Raphael, M. (2007). Interannual variability associated with semiannual oscillation in southern high latitudes. *Journal of Geophysical Research: Atmospheres*, *112*(D2). doi: 10.1029/2006JD007648

Turner, J., Bracegirdle, T. J., Phillips, T., Marshall, G. J., & Hosking, J. S. (2013). An initial assessment of antarctic sea ice extent in the CMIP5 models. *Journal of Climate*, *26*(5), 1473-1484. doi: 10.1175/JCLI-D-12-00068.1

Van Den Broeke, M. (2000). The semi-annual oscillation and antarctic climate. part 4: a note on sea ice cover in the amundsen and bellingshausen seas. *International Journal of Climatology*, *20*(4), 455-462. doi: 10.1002/(SICI)1097-0088(20000330)20:4⟨455::AID-JOC482⟩3.0.CO;2-M

van Loon, H. (1967). The half-yearly oscillations in middle and high southern latitudes and the coreless winter. *Journal of the Atmospheric Sciences*, *24*(5), 472-486. doi: 10.1175/1520-0469(1967)024⟨0472:THYOIM⟩2.0.CO;2

Van Loon, H., & Rogers, J. C. (1984). Interannual variations in the half-yearly cycle of pressure gradients and zonal wind at sea level on the southern hemisphere. *Tellus A*, *36A*(1), 76-86. doi: 10.1111/j.1600-0870.1984.tb00224.x

Yuan, X., & Martinson, D. (2000, 05). Antarctic sea ice extent variability and its global connectivity*. *Journal of Climate*. doi: 10.1175/1520-0442(2000)013⟨1697:ASIEVA⟩2.0.CO;2

Yuan, X., & Martinson, D. G. (2001). The antarctic dipole and its predictability. *Geophysical Research Letters*, *28*(18), 3609-3612. Retrieved from `https://agupubs.onlinelibrary.wiley.com/doi/abs/10.1029/2001GL012969` doi: 10.1029/2001GL012969

Figure 01a.

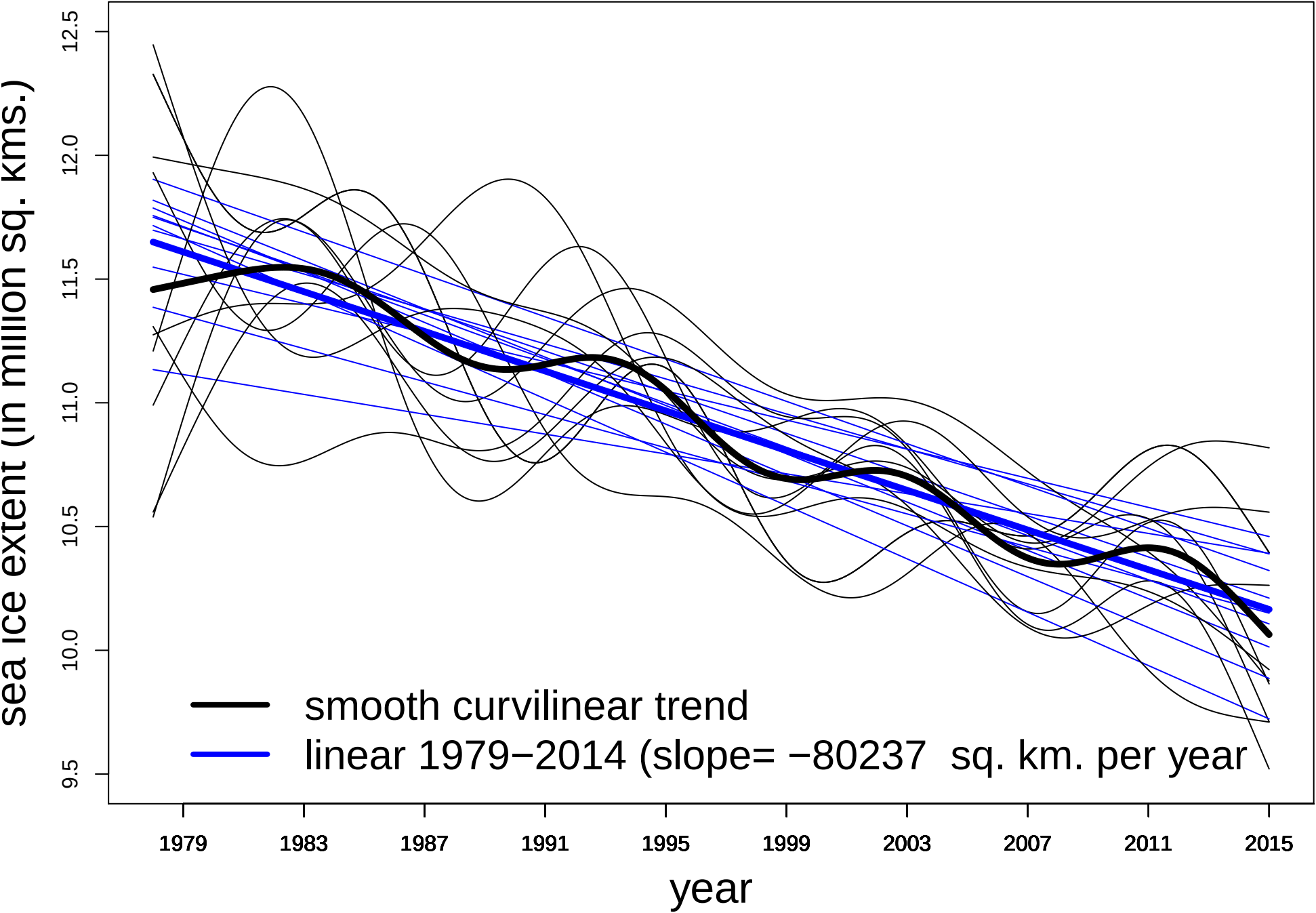
sea ice extent (in million sq. kms.)
12.5
12.0
11.5
11.0
10.5
10.0
9.5
1979
1983
1987
1991
1995
1999
2003
2007
2011
2015
year
smooth curvilinear trend
linear 1979−2014 (slope= −80237 sq. km. per year

Figure 01b.

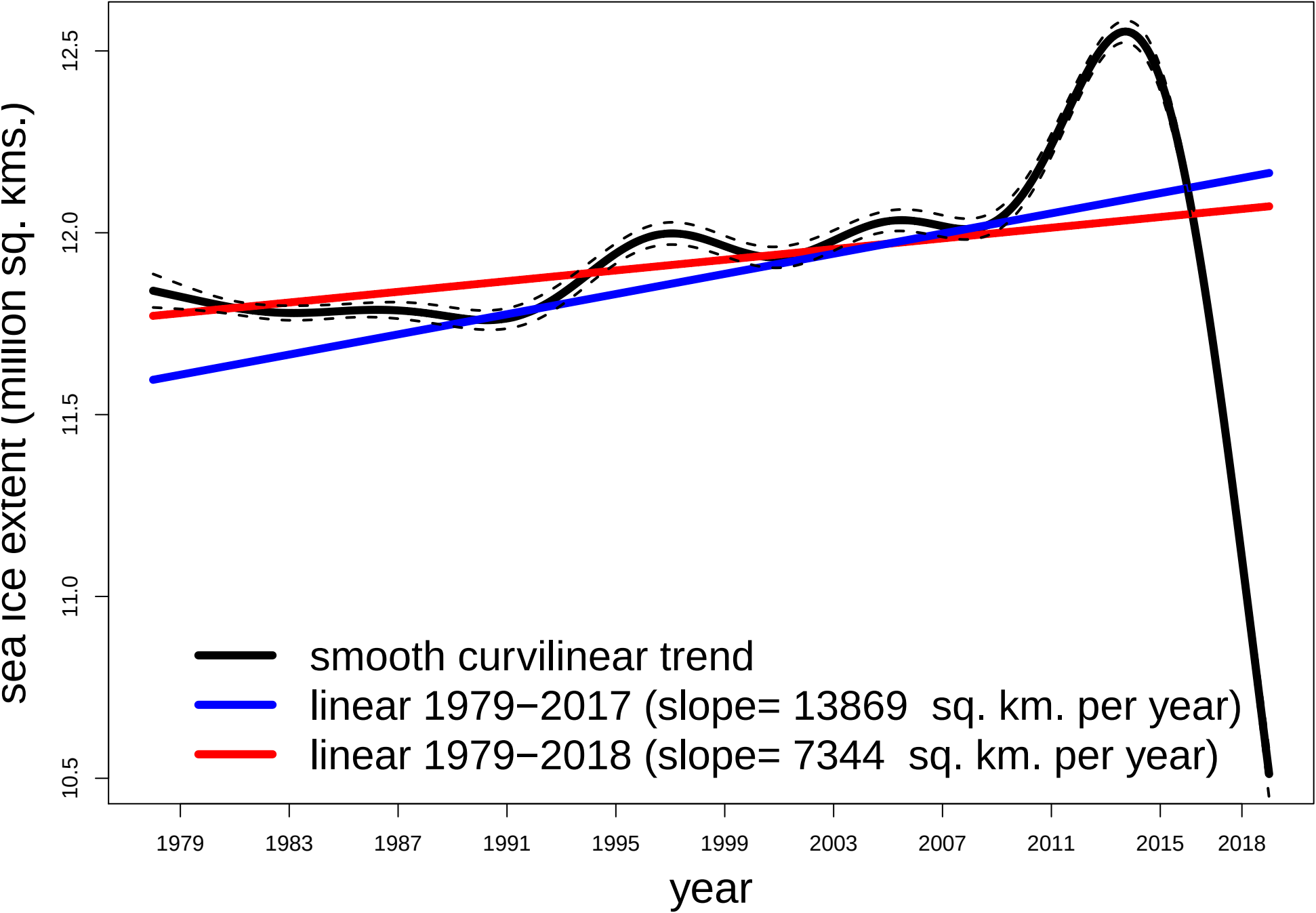
sea ice extent (million sq. kms.)
12.5
12.0
11.5
11.0
10.5
1979
1983
1987
1991
1995
1999
2003
2007
2011
2015
2018
year
smooth curvilinear trend
linear 1979−2017 (slope= 13869 sq. km. per year)
linear 1979−2018 (slope= 7344 sq. km. per year)

Figure 02a.

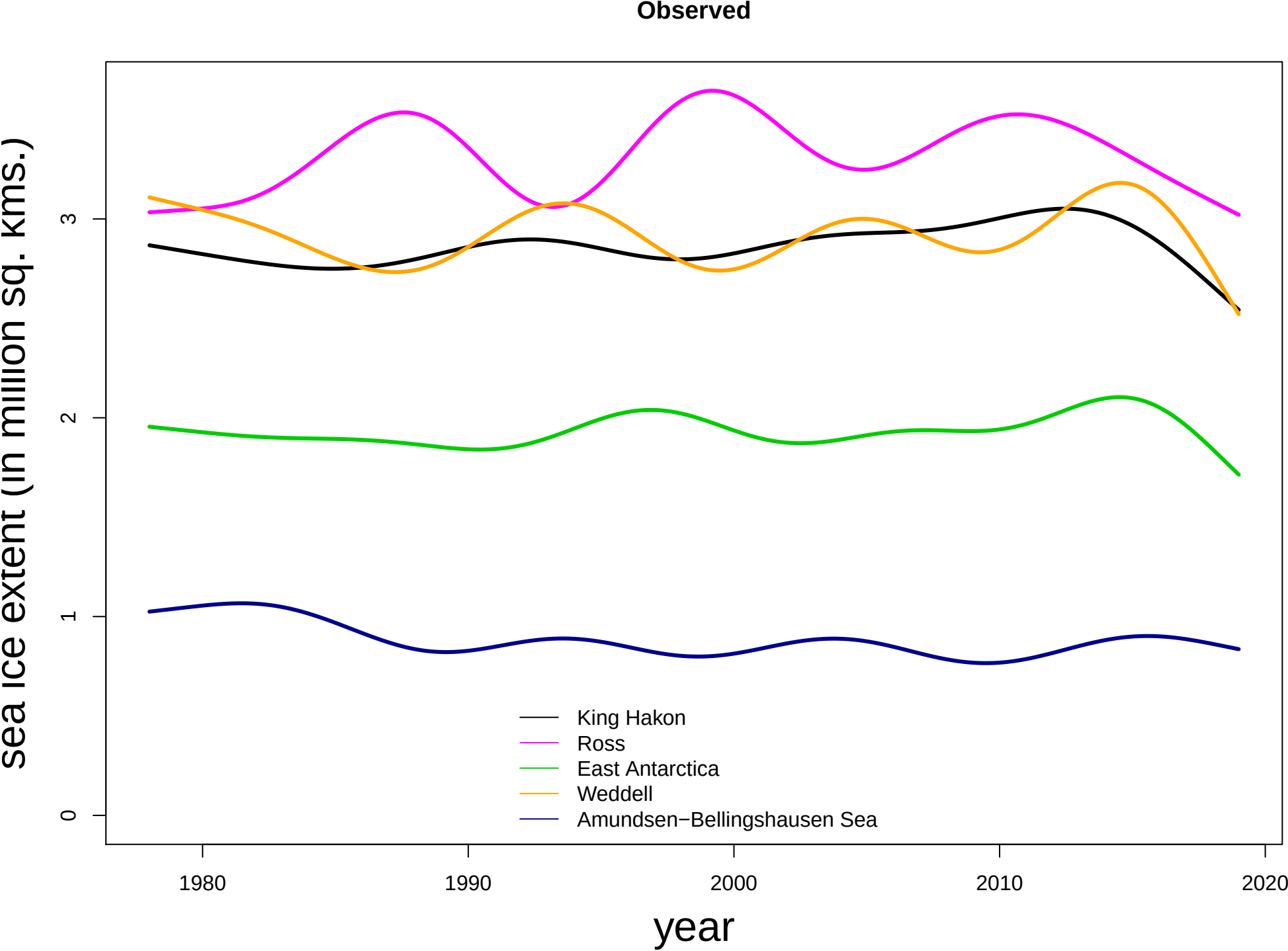
Observed
sea ice extent (in million sq. kms.)
0
1
2
3
1980
1990
2000
2010
2020
year
King Hakon
Ross
East Antarctica
Weddell
Amundsen−Bellingshausen Sea

Figure 02b.

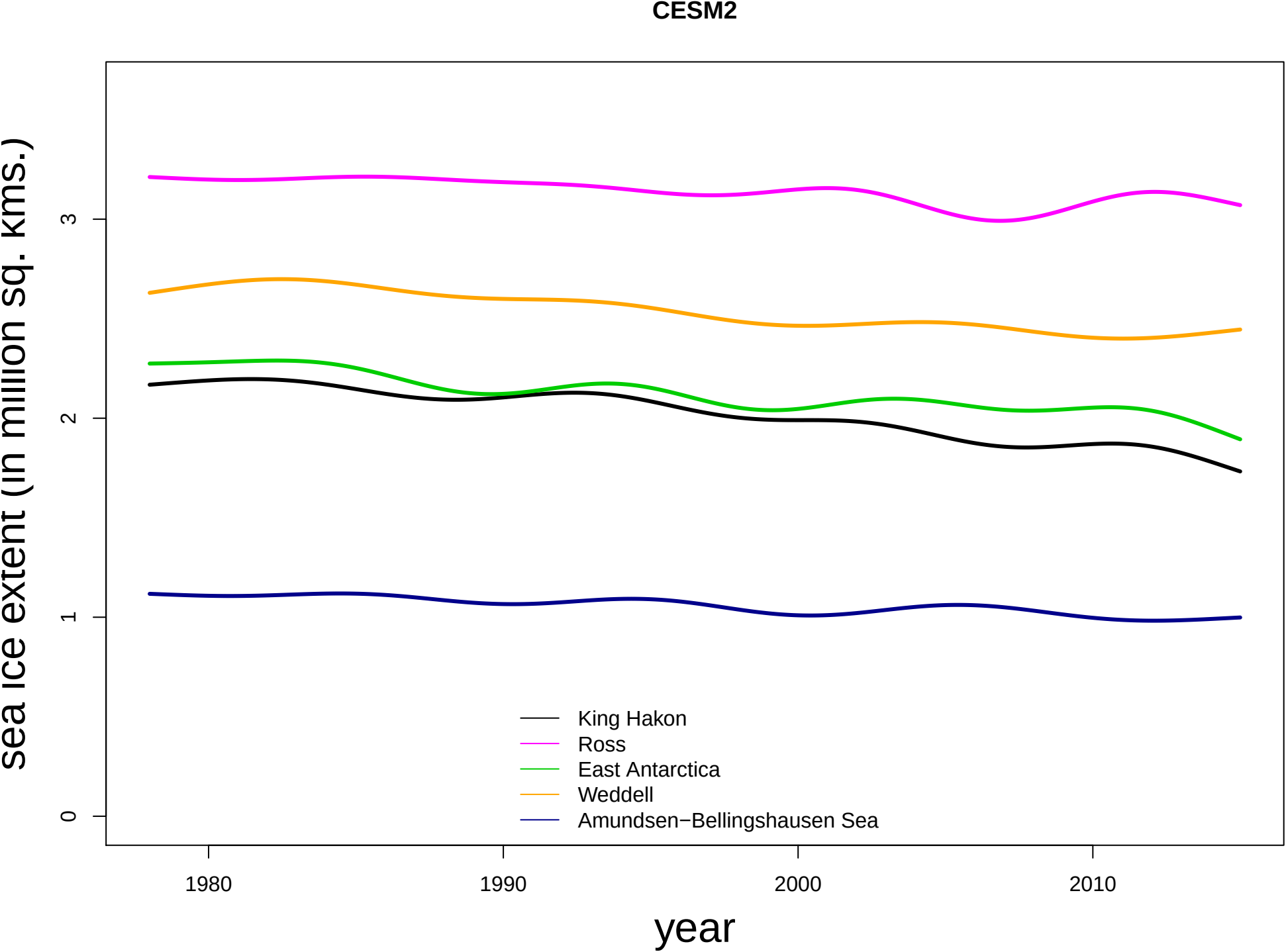
CESM2
sea ice extent (in million sq. kms.)
0
1
2
3
1980
1990
2000
2010
year
King Hakon
Ross
East Antarctica
Weddell
Amundsen−Bellingshausen Sea

Figure 03.

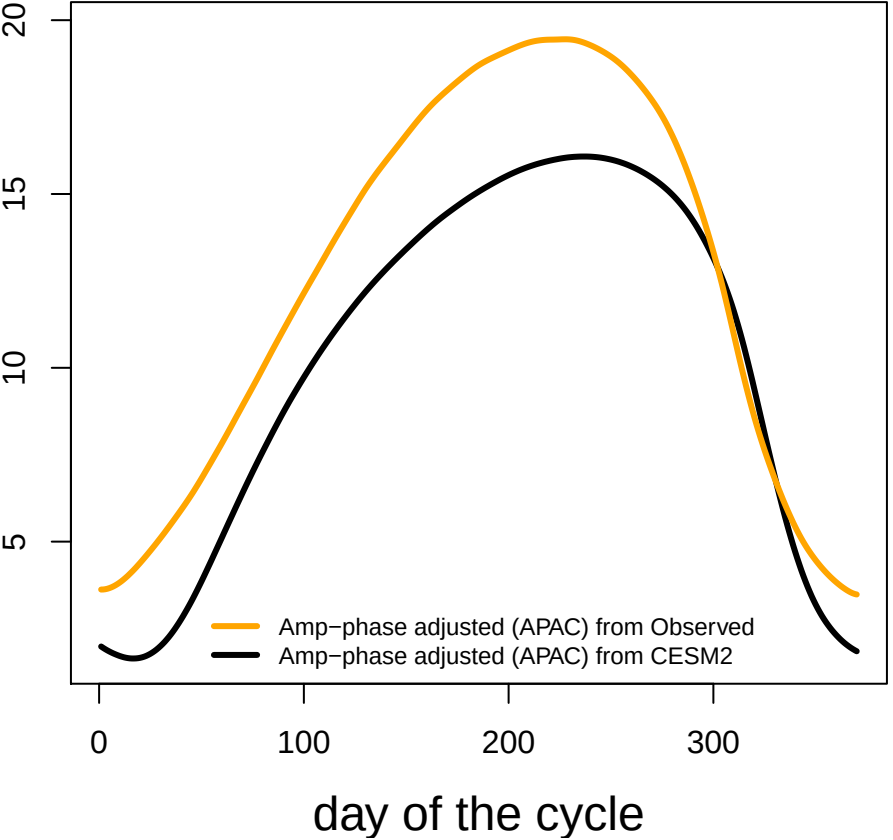
Amp−phase adjusted (APAC) from Observed
Amp−phase adjusted (APAC) from CESM2
5
10
15
20
0
100
200
300
day of the cycle

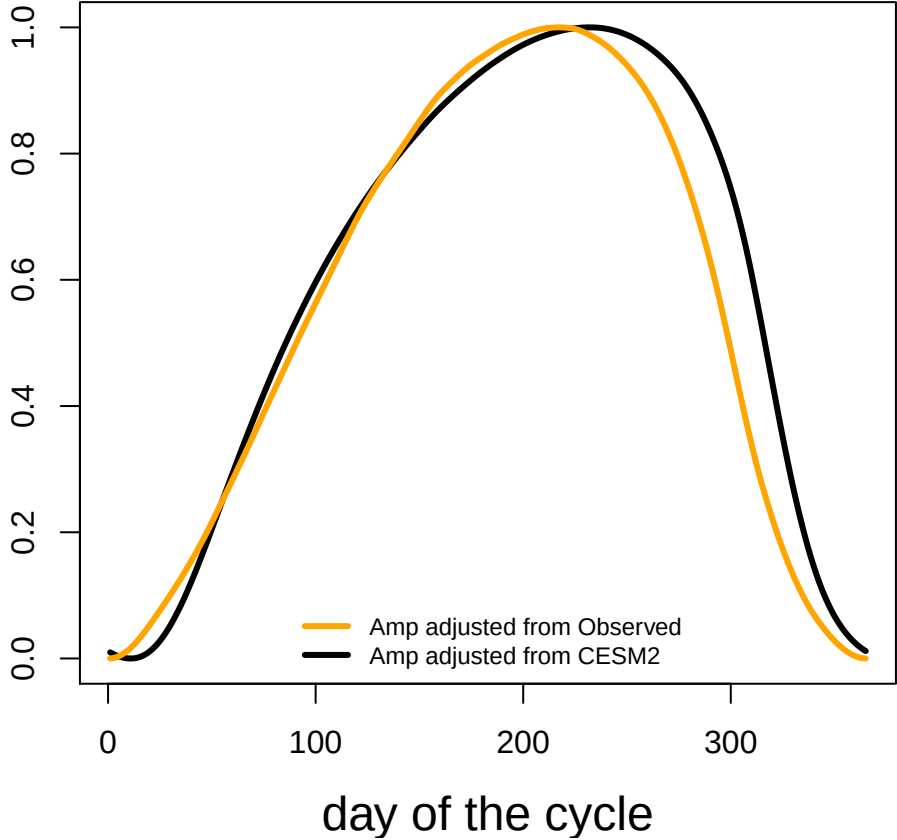
Amp adjusted from Observed
Amp adjusted from CESM2
0.0
0.2
0.4
0.6
0.8
1.0
0
100
200
300
day of the cycle

Figure 04.

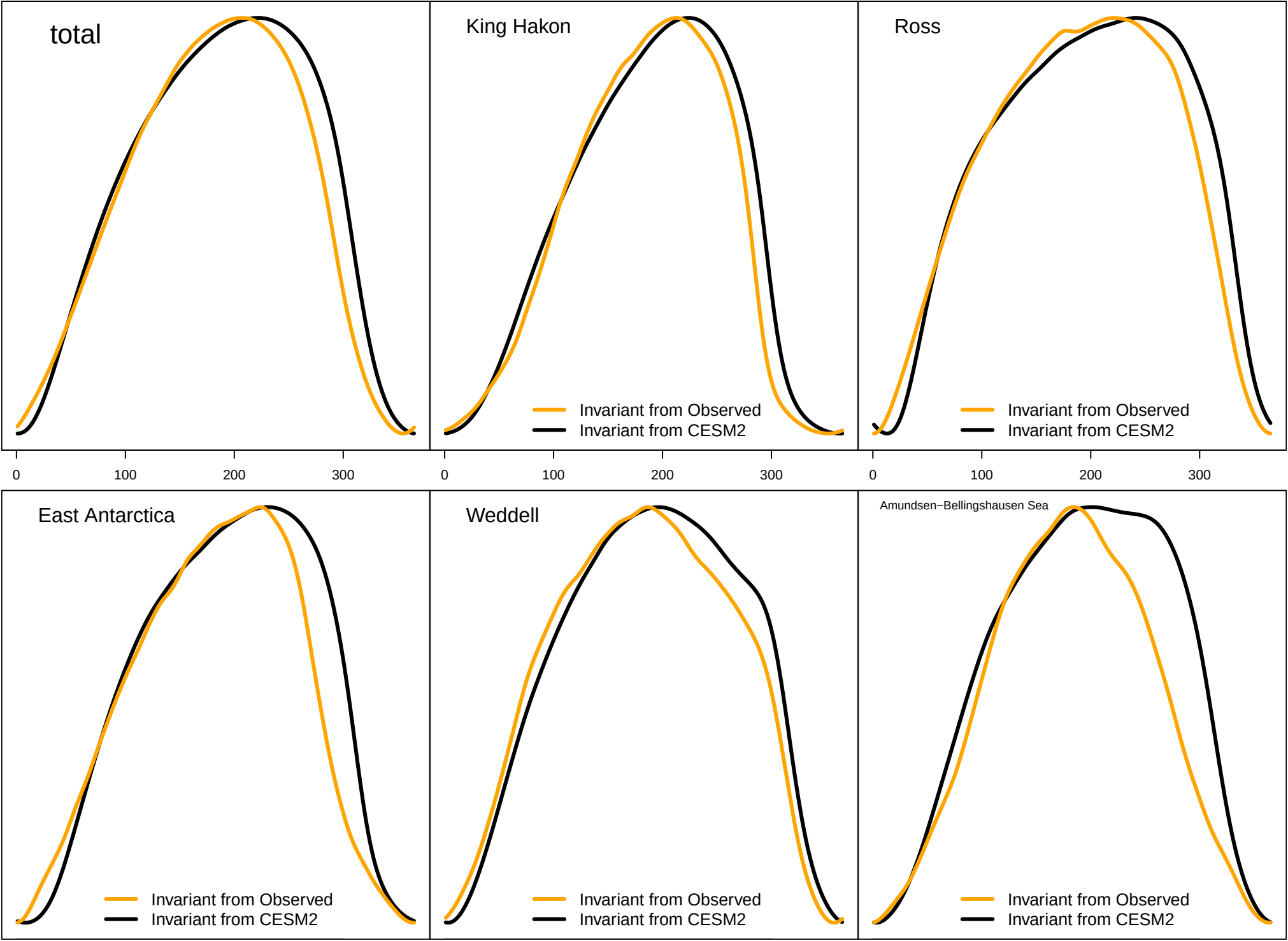
total
King Hakon
Ross
East Antarctica
Weddell
Amundsen−Bellingshausen Sea
Invariant from Observed
Invariant from CESM2
0
100
200
300

Figure 05.

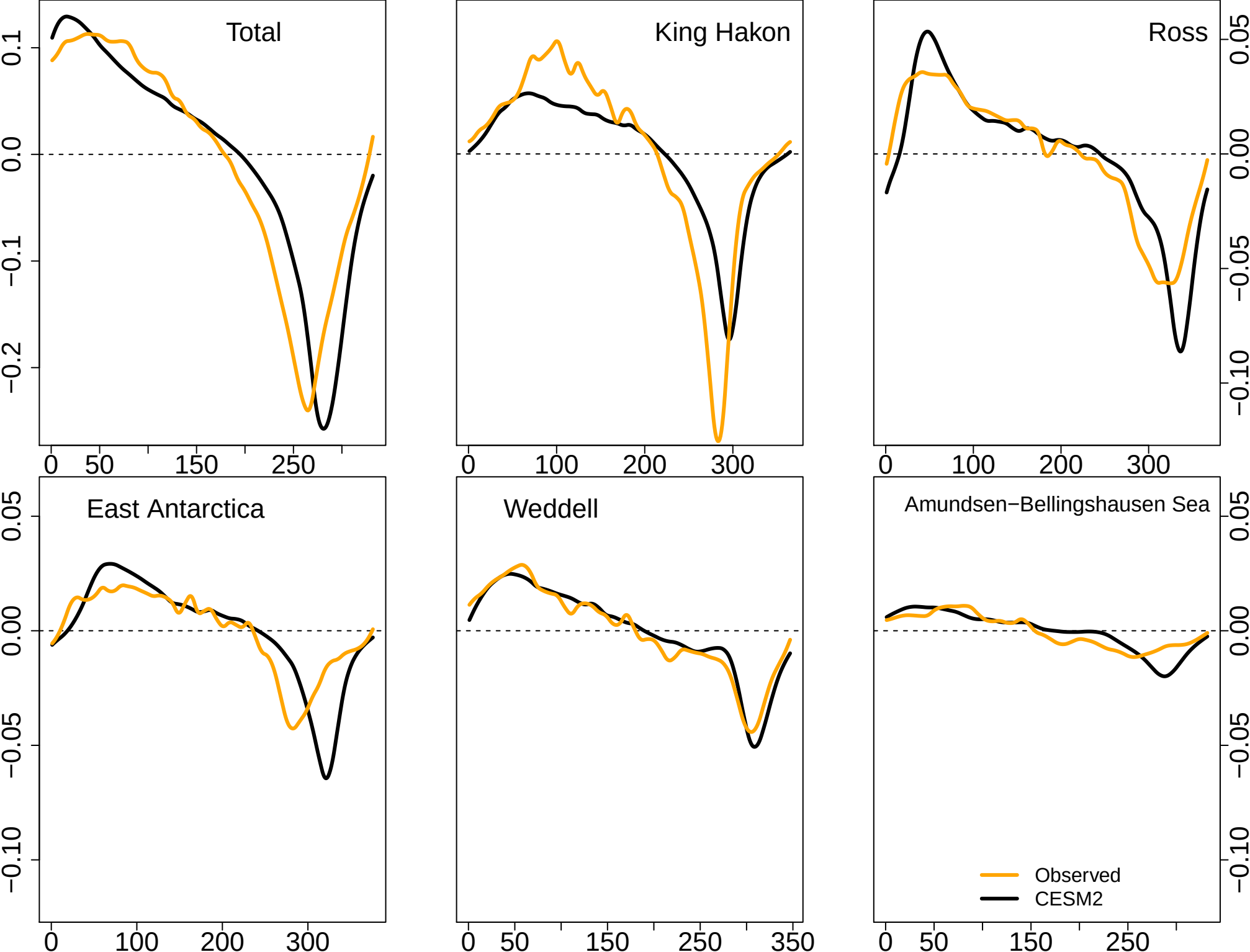
Total
King Hakon
Ross
East Antarctica
Weddell
Amundsen−Bellingshausen Sea
Observed
CESM2

Figure 06.

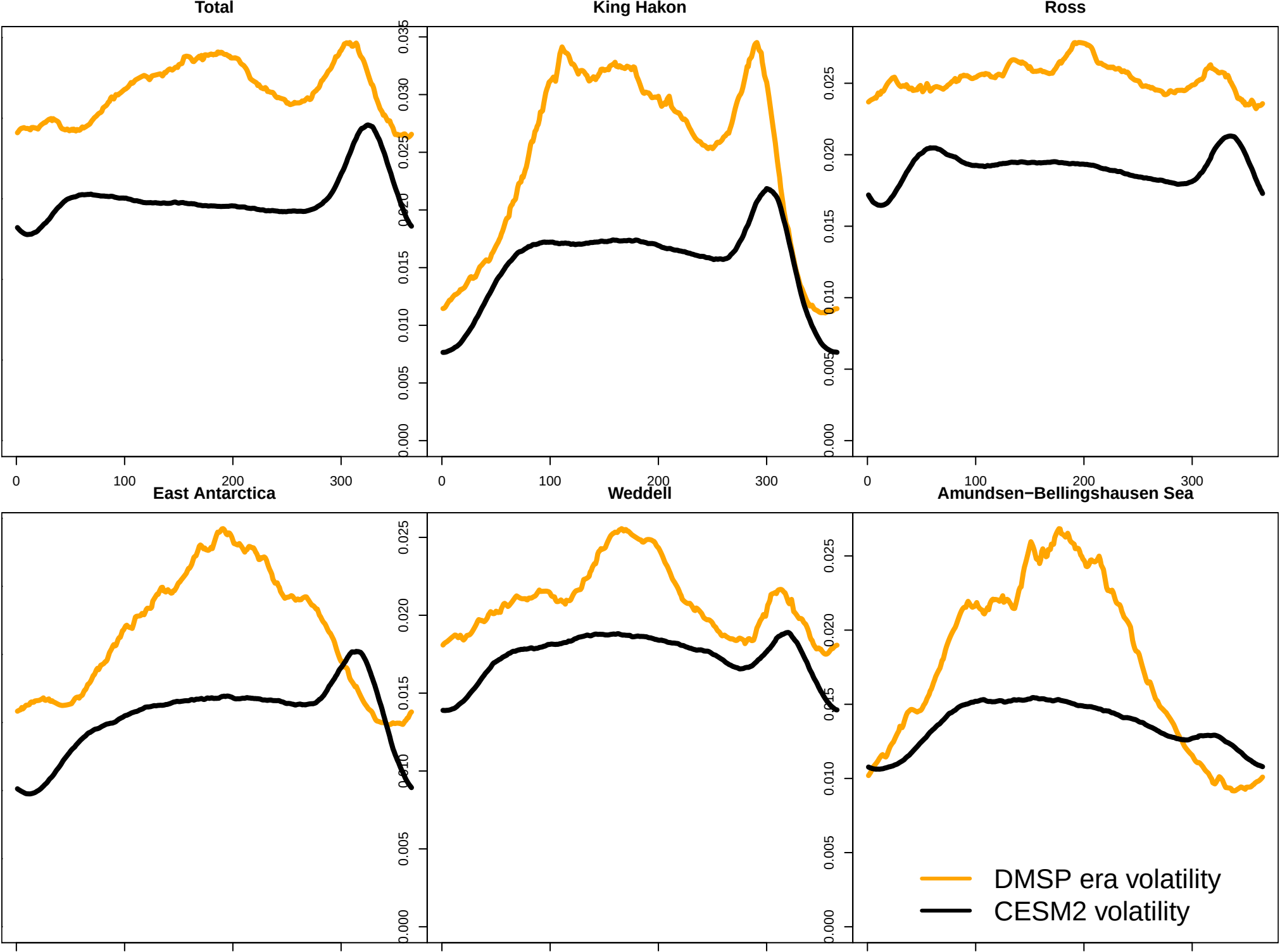
Total
King Hakon
Ross
East Antarctica
Weddell
Amundsen−Bellingshausen Sea
0.000
0.005
0.010
0.015
0.020
0.025
0.030
0.035
0
100
200
300
DMSP era volatility
CESM2 volatility

Figure 07.

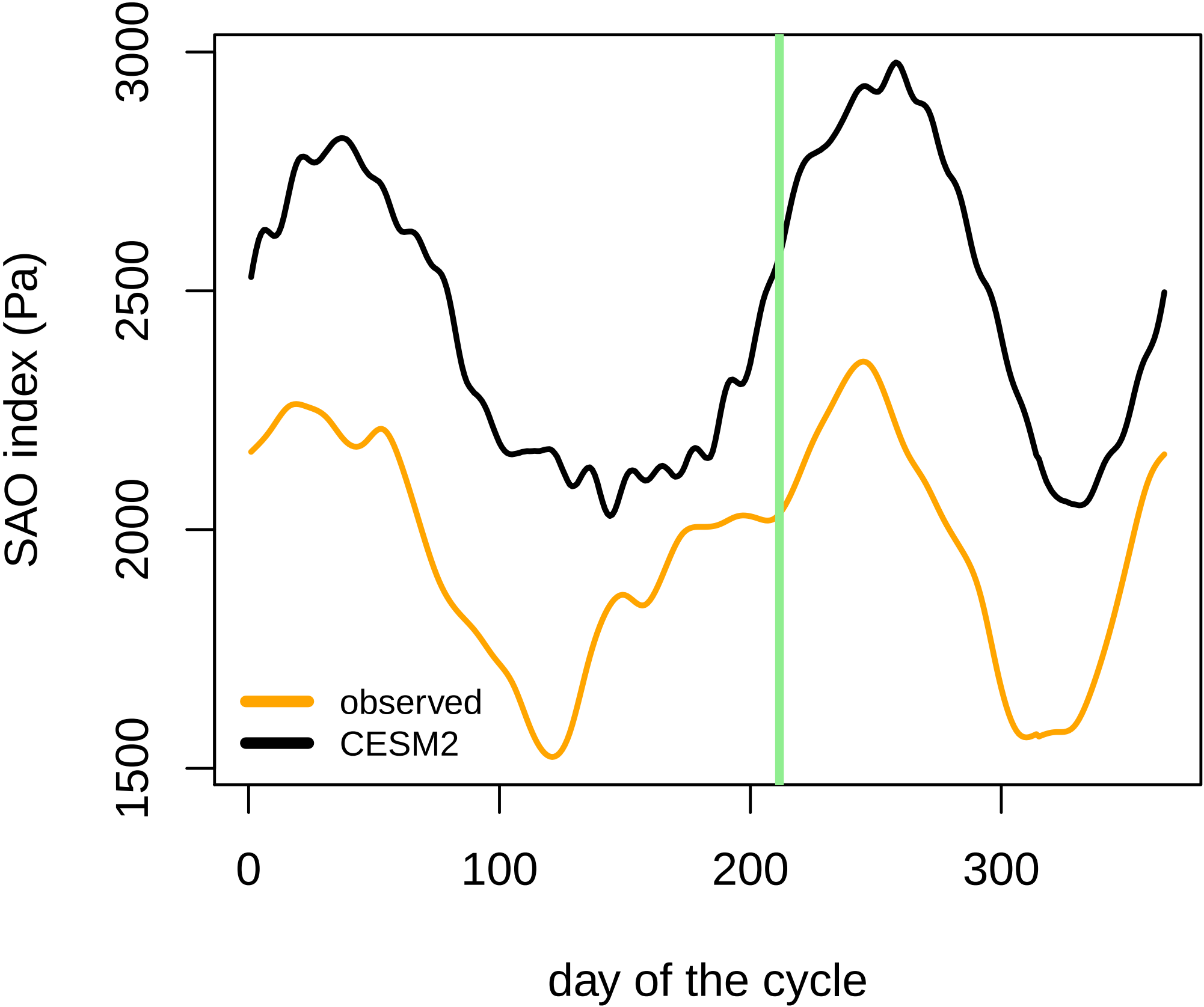
SAO index (Pa)
1500
2000
2500
3000
0
100
200
300
day of the cycle
observed
CESM2

Figure 08.

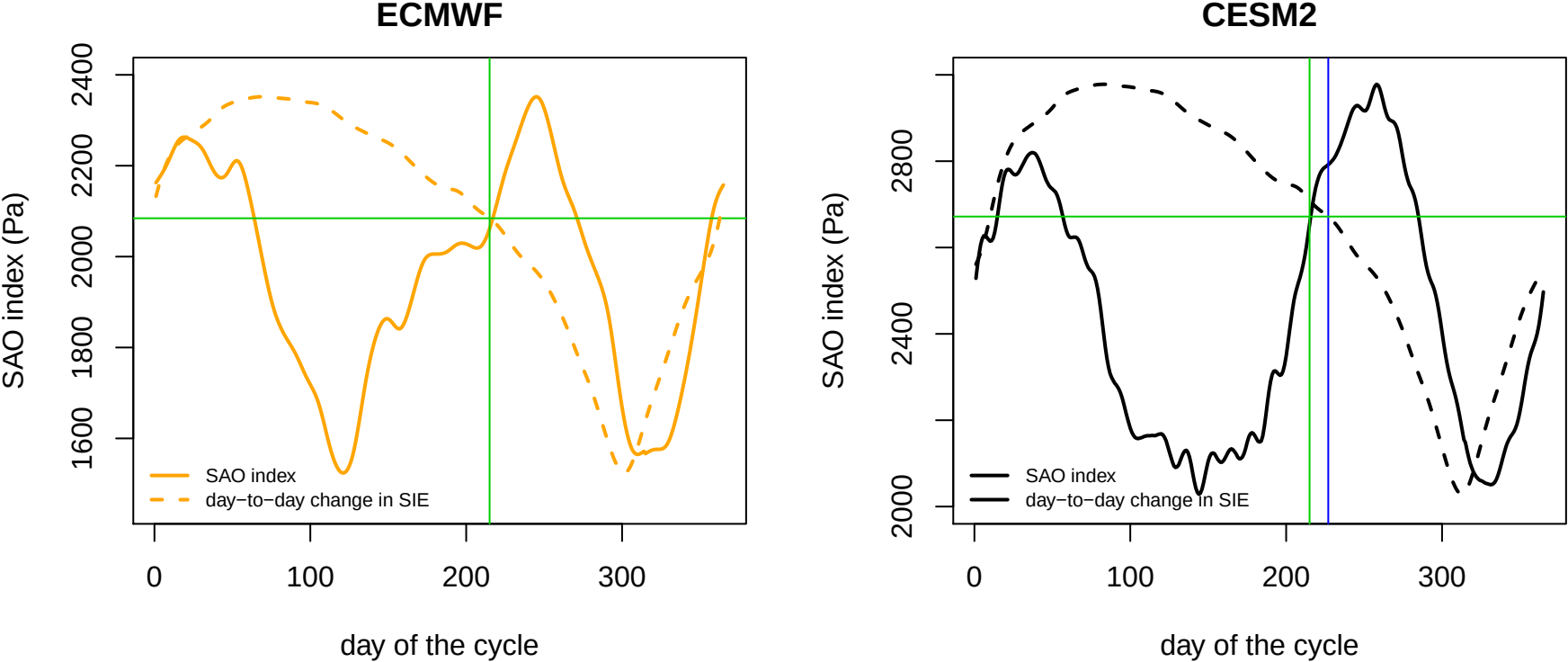
ECMWF
SAO index (Pa)
1600
1800
2000
2200
2400
SAO index
day−to−day change in SIE
0
100
200
300
day of the cycle
CESM2
SAO index (Pa)
2000
2400
2800
SAO index
day−to−day change in SIE
0
100
200
300
day of the cycle

Figure Regions.

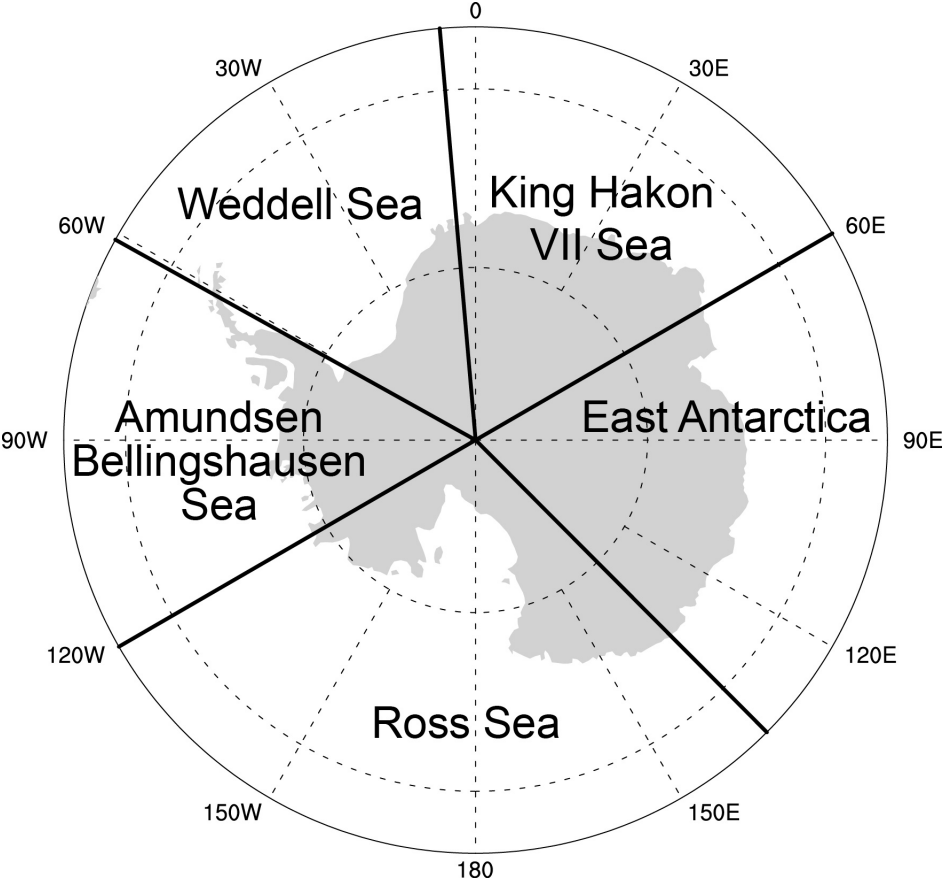
0
30W
30E
60W
60E
90W
90E
120W
120E
150W
150E
180
Weddell Sea
King Hakon VII Sea
Amundsen Bellingshausen Sea
East Antarctica
Ross Sea